

# Single-mode low-loss optical fibers for long-wave infrared transmission

Zhiyong Yang,<sup>1</sup> Tao Luo,<sup>2</sup> Shibin Jiang,<sup>2</sup> Jihong Geng,<sup>2</sup> and Pierre Lucas<sup>1,\*</sup>

<sup>1</sup>Department of Materials Science and Engineering, University of Arizona, Tucson, Arizona 85712, USA

<sup>2</sup>AdValue Photonics, 4585 S. Palo Verde Road, Suite 405, Tucson, Arizona 85714, USA

\*Corresponding author: pierre@email.arizona.edu

Received July 27, 2010; revised August 31, 2010; accepted September 2, 2010;  
posted September 20, 2010 (Doc. ID 132364); published October 8, 2010

In this Letter, we report single-mode fibers made of chalcogenide glasses with low loss in the 5–12  $\mu\text{m}$  range. Glasses from the Ge–As–Te–Se system were optimized to prevent nucleation and to exhibit low density of charge carriers. Single-mode fibers were obtained through the rod-in-tube method by substituting 2% Te/Se between the core and cladding glasses. The resulting single-mode fibers had a core diameter of 30  $\mu\text{m}$  and exhibited losses of  $\sim 6$  dB/m at 10.6  $\mu\text{m}$ , and as low as 3–4 dB/m in the 6–10  $\mu\text{m}$  range. © 2010 Optical Society of America

OCIS codes: 060.2280, 060.2390, 060.2430, 160.2750.

Single-mode fibers with high transparency in the mid-IR have many important applications, ranging from biosensing to thermal imaging or space exploration. For example, these fibers can enable the remote detection of the so-called “signature region” of biomolecules in the 5–12  $\mu\text{m}$  range by using evanescent wave spectroscopy [1] and are also ideal for laser communication or optical detection within the second atmospheric window at 8–12  $\mu\text{m}$ . Additionally, they have good potential for thermal imaging of blackbody radiation near 10  $\mu\text{m}$  or for CO<sub>2</sub> laser delivery at 10.6  $\mu\text{m}$  [2]. Finally, there has recently been much interest in using these fibers as modal filters in nulling interferometry for the detection of molecular signals from exoplanets as part of the DARWIN or Terrestrial Planet Finder programs [3,4].

While mid-IR single-mode fibers have been previously obtained by extrusion of polycrystalline silver halide [5–7], this material suffers from photodegradation and inferior chemical durability [8]. The polycrystalline extrusion process also generates a poor core/cladding interface, which results in losses of 20–40 dB/m in the 8–12  $\mu\text{m}$  range [7]. In contrast, chalcogenide glasses exhibit outstanding rheological properties and can be easily drawn or molded into high-quality optical elements by heating above the glass transition temperature. For double index fibers, the standard rod-in-tube method leads to smooth core/cladding interfaces and perfectly circular symmetry, which lend themselves well to the production of single-mode fibers. Chalcogenide glasses can also be synthesized in extremely high purity and can reach losses as low as 12 dB/km [9]. Many dozens of meters of homogeneous fibers can be drawn from a single preform.

Most chalcogenide glasses are based on sulfur and selenium, and single-mode fibers have been previously obtained with these glasses [10,11]; however, the higher phonon energies associated with low-mass constituents result in transparency cutoff between 6 and 9  $\mu\text{m}$ . In contrast, tellurium glasses have lower phonon energies and result in wider optical windows [12–14], but the metallic character of Te leads to a greater tendency for crystallite formation, which prevents the production of low-loss optical fibers due to scattering effects. A second consequence of the metallic character of Te is a low bandgap that results in significant background carrier ab-

sorption due to thermally excited charge carriers at room temperature [15]. However, these drawbacks can be alleviated by the substitution of a small amount of Te by Se, which both lowers the conductivity and dramatically increases the resistance to crystallization while retaining a wide optical window to long wavelengths. Here we report the realization of single-mode fibers with low losses in the 5–12  $\mu\text{m}$  range.

It was previously shown that glasses from the Ge–As–Te system can be produced over a wide compositional range [14], including Te-rich glasses containing up to 80% tellurium. While these glasses exhibit outstanding optical windows, they suffer from small values of  $\Delta T = T_g - T_x$  (where  $T_x$  is the recrystallization temperature and  $T_g$  is the glass transition temperature), which prevents the easy formation of crystallite-free fibers. The  $\Delta T$  parameter constitutes a measure of the suitability of a glass for fiber drawing and a  $\Delta T > 120$  °C is usually required to minimize risks of crystallization during the drawing process.

Figure 1 shows typical differential scanning calorimetry (DSC) curves of glasses in Ge–As–Te and Ge–As–Te–Se systems. The addition of  $\sim 15\%$  Se to the mixture results in far greater stability toward crystallization. The crystallization peak has effectively disappeared from the range of

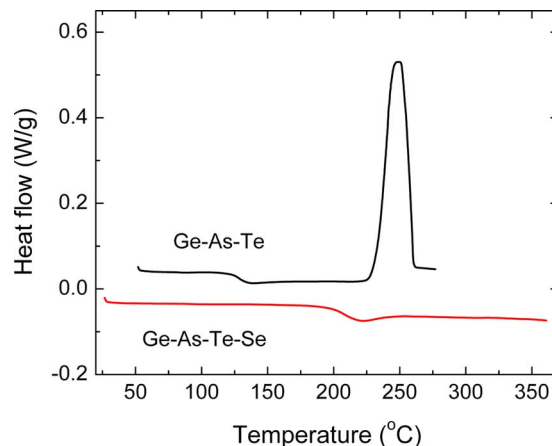


Fig. 1. (Color online) Differential scanning calorimetry trace of Ge<sub>20</sub>As<sub>20</sub>Te<sub>45</sub>Se<sub>15</sub> glass compared to that of Ge<sub>10</sub>As<sub>15</sub>Te<sub>75</sub> glass.

temperature of interest for fiber drawing, therefore allowing the production of structurally and optically homogeneous glass fibers with minimal scattering losses. In comparison, the scattering losses in the Ge–As–Te fibers were so large that an attenuation curve could not be obtained. Another notable advantage of selenium substitution is a significant increase in bandgap energy, which considerably decreases the population of thermally excited charge carriers. As a consequence, the room temperature conductivity decreases by 3 orders of magnitude from  $10^{-5}$  to  $10^{-8}(\Omega\cdot\text{cm})^{-1}$  upon selenium substitution. This effectively reduces the density of free-charge carriers, which are known to produce significant background losses analogous to Ge semiconductors [15].

To produce high-purity glasses for low-loss waveguide fabrication, 6N purity elements were introduced in a silica tube under  $10^{-6}$  Torr vacuum and purified *in situ* to eliminate high vapor pressure impurities, such as Se–O surface oxides. The mixture was then combined with Al oxygen-getter and distilled in order to remove remaining traces of low vapor pressure contaminants. The glass was then sealed under vacuum and homogenized in a rocking furnace at 800 °C for 12 h. After quenching, the resulting glass rod was annealed at around  $T_g$  for 3 h. For double-index fiber drawing, core/cladding preforms were produced by synthesizing two rods with slightly different compositions. The substitution of 2% tellurium by selenium was sufficient to generate an adequate refractive index contrast for single-mode fiber fabrication. The core glass had a composition of  $\text{Ge}_{20}\text{As}_{20}\text{Te}_{44}\text{Se}_{16}$  and a refractive index  $n_{\text{co}} = 3.025$  at  $10.6\ \mu\text{m}$  measured by specular reflectance [11]. The cladding glass had a composition of  $\text{Ge}_{20}\text{As}_{20}\text{Te}_{42}\text{Se}_{18}$  and a refractive index  $n_{\text{cl}} = 3.014$  at  $10.6\ \mu\text{m}$ . The maximum core diameter required to obtain single-mode propagation for this specific refractive index contrast can be obtained from Eq. (1) [5]:

$$V = \frac{2\pi\rho}{\lambda} \sqrt{n_{\text{co}}^2 - n_{\text{cl}}^2}, \quad (1)$$

where  $\rho$  is the core radius and  $\lambda$  is the propagating light wavelength. Single-mode propagation is obtained for  $V < 2.405$ . In the present case, this implies a maximum core diameter of  $32\ \mu\text{m}$  for propagation of  $10.6\ \mu\text{m}$  light. Preforms with adequate size ratio were produced by drilling a 2 mm diameter hole into a 10 mm diameter cladding glass and reducing a core rod to 2 mm diameter using the drawing tower. The inner surface of the cladding tube was polished using abrasive  $\text{Al}_2\text{O}_3$ . The core rod was then inserted in the polished cladding tube and drawn into fibers of different diameters.

Figure 2 represents the  $\text{CO}_2$  laser output images of a series of core/cladding fibers with core diameter ranging from 60 to  $30\ \mu\text{m}$  ( $d_{\text{clad}}/d_{\text{core}} = 5$ ). The output images were obtained by launching a  $\text{CO}_2$  laser with a perfect Gaussian profile into one end of a 2.5-m-long fiber using a ZnSe lens. The lens was adjusted to focus the laser within the fiber core. The output light was then projected on a screen placed a few centimeters away from the fiber output end and imaged using a Fluke TiR2 IR camera. The fiber was coated with gallium to remove the cladding modes. Figure 2 clearly indicates that the fibers with core

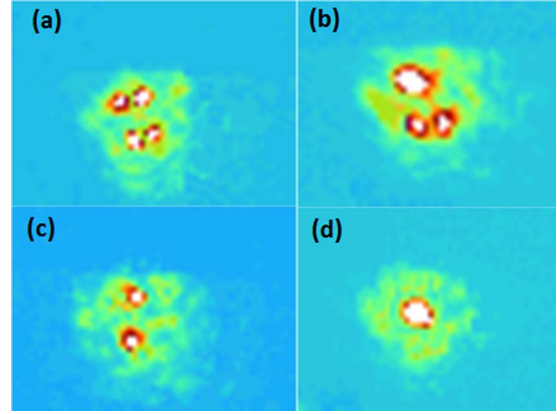


Fig. 2. (Color online) Output images of a series of core/cladding Ge–As–Te–Se glass fibers with various core diameters  $d_{\text{core}}$  ( $d_{\text{clad}}/d_{\text{core}} = 5$ ): (a)  $d_{\text{core}} = 60\ \mu\text{m}$ , (b)  $d_{\text{core}} = 50\ \mu\text{m}$ , (c)  $d_{\text{core}} = 40\ \mu\text{m}$ , (d)  $d_{\text{core}} = 30\ \mu\text{m}$ .

diameter larger than  $32\ \mu\text{m}$  propagate several modes simultaneously. The fiber with core diameter  $d = 60\ \mu\text{m}$  propagates four modes [Fig. 2(a)], while the fibers with core diameter  $d = 50\ \mu\text{m}$  and  $d = 40\ \mu\text{m}$  propagate three modes and two modes, respectively [Fig. 2(b) and 2(c)]. Finally, Fig. 2(d) indicates that the fiber with a total diameter of  $150\ \mu\text{m}$  and a core diameter of  $30\ \mu\text{m}$  propagates only a single mode as expected from the measured refractive index contrast between the core and the cladding. This single-mode fiber has a cutoff wavelength of  $10.0\ \mu\text{m}$ , where the  $V$  number is 2.405. The  $\text{CO}_2$  laser corresponds to a  $V$  number of 2.290 and has a mode-field diameter of  $34\ \mu\text{m}$  in the fiber.

The transmission losses were also estimated at  $10.6\ \mu\text{m}$  using the cutback method. The output power was measured using an Ophir power meter before and after several 30-cm-long pieces of fiber were cleaved off the fiber end. The attenuation measured this way yielded a loss of  $\sim 6\ \text{dB/m}$  at  $10.6\ \mu\text{m}$ . The fiber started to be damaged as the input  $\text{CO}_2$  power intensity reached  $\sim 35\ \text{kW/cm}^2$  without any assistant cooling. In addition, the fiber attenuation over the whole range of wavelength from 5 to  $12\ \mu\text{m}$  was measured using a Fourier transform IR (FTIR) spectrometer Bruker Tensor 27 equipped with a fiber coupler composed of gold-coated concave mirrors. The focusing diameter was larger than the fiber core; hence, the fiber was coated with gallium in order to remove the cladding modes. The attenuation was measured on a 1.2-m-long fiber using the cutback method by removing 20 cm sections of fibers. Figure 3 shows the losses measured on a core/cladding single-mode fiber with core diameter of  $30\ \mu\text{m}$ . This fiber exhibits a loss of  $5.5\ \text{dB/m}$  at  $10.6\ \mu\text{m}$  and losses as low as 3–4 dB/m in the 6–10  $\mu\text{m}$  range. The inset in Fig. 3 displays an optical micrograph of the fiber that emphasizes the high surface quality obtained during drawing. The losses may be caused by the intrinsic absorptions (including the absorptions of free carriers) of the materials, the scattering resulting from microinhomogeneity in the glass, and imperfect interfaces between the core and cladding. The lowest loss of Ge–As–Te–Se fibers was reported on an unclad single-index fiber [16]. The unclad fiber ( $\text{Ge}_{30}\text{As}_{10}\text{Se}_{30}\text{Te}_{30}$ ) showed losses of  $\sim 1\ \text{dB/m}$  between 5 and  $9\ \mu\text{m}$  and  $\sim 2\ \text{dB/m}$  at  $10.6\ \mu\text{m}$ . It is possible to reduce the loss of

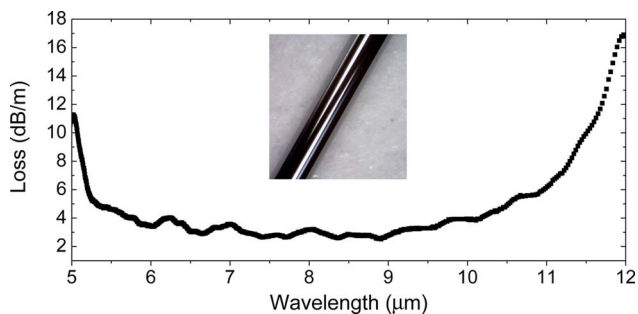


Fig. 3. Attenuation of a single-mode Ge-As-Te-Se fiber in the 5–12  $\mu\text{m}$  range; the inset is an optical micrograph of the fiber 150  $\mu\text{m}$  in diameter.

our single-mode fiber by improved purification, composition optimization, and better control of parameters in the fiber drawing. Among reported chalcogenide single-mode fibers, Te-As-Se fiber [11] showed the lowest loss of  $\sim 10$  dB/m at 10.6  $\mu\text{m}$ , which was mainly caused by multiphonon absorptions of the glass. In comparison, our single-mode fiber exhibits a lower loss at 10.6  $\mu\text{m}$ . Hollow bandgap fibers could also be designed to transmit IR lights around 10  $\mu\text{m}$  with low loss ( $\sim 1$  dB/m) [17], but they could transmit only a narrow wavelength range, depending on the fundamental photonic bandgap, and they need state-of-the-art fabrication techniques.

In summary, it was shown that low-loss single-mode fibers can be obtained using stable chalcogenide glasses in the Ge-As-Te-Se system. A 2% variation in Se/Te content was sufficient to produce a refractive index contrast between the core and cladding glass that allowed single-mode propagation at 10.6  $\mu\text{m}$  with a core diameter of 30  $\mu\text{m}$ . The losses measured using the cutback method with a  $\text{CO}_2$  laser or with an FTIR spectrometer were consistent and revealed a loss of  $\sim 6$  dB/m at 10.6  $\mu\text{m}$  and losses as low as 3–4 dB/m in the 6–10  $\mu\text{m}$  range.

This work was mainly supported by U.S. Department of Energy (DOE) SBIR project DE-SC0000972 managed by Victoria T. Franques. The authors acknowledge the

technical support of Norm Anheier from Pacific Northwest National Laboratory. The authors thank National Science Foundation (NSF) grants ECCS-0901069 and DMR-0806333 for financial support.

## References

1. P. Lucas, M. R. Riley, C. Boussard-Plédel, and B. Bureau, *Anal. Biochem.* **351**, 1 (2006).
2. Y. Lavi, A. Millo, and A. Katzir, *Appl. Phys. Lett.* **87**, 241122 (2005).
3. G. Lund and H. Bonnet, *C. R. Acad. Sci.* **2**, 137 (2001).
4. L. Kaltenecker and M. Fridlund, *Adv. Space Res.* **36**, 1114 (2005).
5. S. Shalem, A. Tsun, E. Rave, A. Millo, L. Nagli, and A. Katzir, *Appl. Phys. Lett.* **87**, 091103 (2005).
6. T. Lewi, S. Shalem, A. Tsun, and A. Katzir, *Appl. Phys. Lett.* **91**, 251112 (2007).
7. T. Lewi, A. Tsun, A. Katzir, J. Kaster, and F. Fuchs, *Appl. Phys. Lett.* **94**, 261105 (2009).
8. O. Eytan, B. A. Sela, and A. Katzir, *Appl. Opt.* **39**, 3357 (2000).
9. G. E. Snopatin, V. S. Shiryaev, V. G. Plotnichenko, E. M. Dianov, and M. F. Churbanov, *Inorg. Mater.* **45**, 1439 (2009).
10. R. Mossadegh, J. S. Sanghera, D. Schaafsma, B. J. Cole, V. Q. Nguyen, R. E. Miklos, and I. D. Aggarwal, *J. Lightwave Technol.* **16**, 214 (1998).
11. P. Houizot, C. Boussard-Plédel, A. J. Faber, L. K. Cheng, B. Bureau, P. A. Van Nijnatten, W. L. M. Gielesen, J. Pereira do Carmo, and J. Lucas, *Opt. Express* **15**, 12529 (2007).
12. A. A. Wilhelm, Q. C. C. Boussard-Plédel, J. Lucas, B. Bureau, and P. Lucas, *Adv. Mater.* **19**, 3796 (2007).
13. S. Danto, P. Houizot, C. Boussard-Plédel, X. H. Zhang, F. Smektala, and J. Lucas, *Adv. Funct. Mater.* **16**, 1847 (2006).
14. Z. Yang and P. Lucas, *J. Am. Ceram. Soc.* **92**, 2920 (2009).
15. I. Inagawa, S. Moritomo, T. Yamashita, and I. Shiratoni, *Jpn. J. Appl. Phys.* **36**, 2229 (1997).
16. J. S. Sanghera, V. Q. Nguyen, P. C. Pureza, F. H. Kung, R. Miklos, and I. D. Aggarwal, *J. Lightwave Technol.* **12**, 737 (1994).
17. B. Temelkuran, S. D. Hart, G. Benoit, J. D. Joannopoulos, and Y. Fink, *Nature* **420**, 650 (2002).